

Supporting Information

Insights into the heterogeneous distribution of SERS effect in plasmonic hot spots between Au@SiO₂ monolayer film and gold single crystal plates

Chao Wei,[†] Chenjie Zhang,[†] Jing Zhang,[†] Minmin Xu,[†] Yaxian Yuan,[†] and Jianlin Yao^{*†}

1. TEM characterization of gold NP seeds

The TEM image of original gold NP seeds is shown in Fig. S1. The average diameter of citrate-reduced torispherical gold NPs is 15 nm, and they have a uniform particle size distribution.

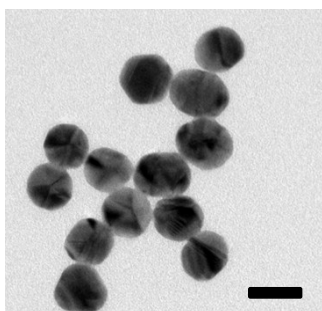


Fig. S1 The TEM image of gold NP seeds . Scale bar: 20 nm.

2. TEM characterizations of (Au-pMBA)@SiO₂ NPs

The TEM images of (Au-pMBA)@SiO₂ NPs with various silica shell thicknesses are shown in Fig. S2. The hydroquinone-reduced two-stepped spherical gold NPs (110 nm) present high uniformity and dispersity which possess good stabilities for the subsequent encapsulation of silica shells.

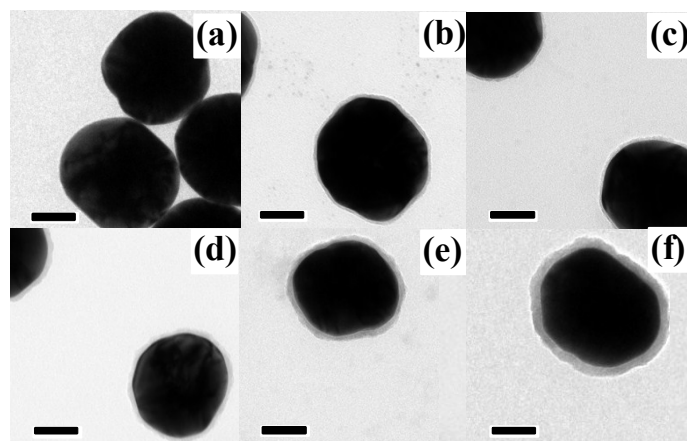
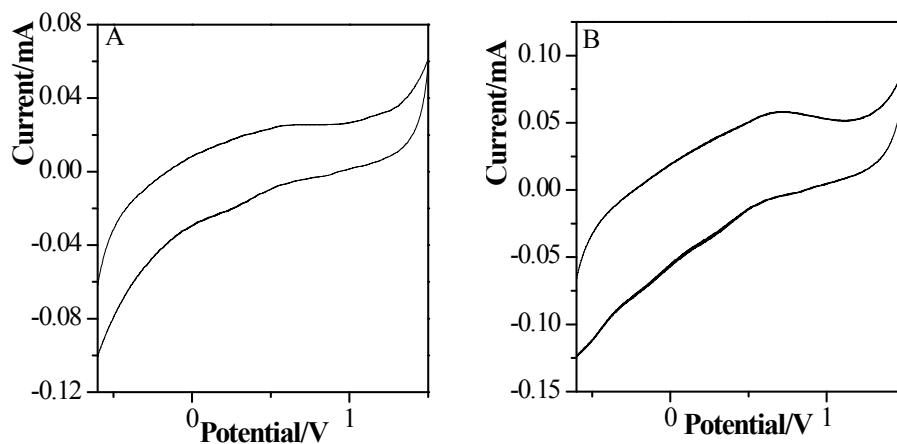


Fig. S2 TEM images of (Au-pMBA) $@\text{SiO}_2$ NPs with the silica thicknesses of 0 nm (naked) (a), 1.8 nm (b), 2.5 nm (c), 5 nm (d), 6.5 nm (e) and 10 nm (f). Scale bar: 50 nm.

3. CV characterizations of (Au-pMBA) $@\text{SiO}_2$ NPs

CV (cyclic voltammetry) technique is often used to measure the completeness of the shells for silica-encapsulated gold CSNPs^{1,2}. Similarly, for our (Au-pMBA) $@\text{SiO}_2$ NPs, this technique can also be introduced in investigating the silica shell continuities of the overall particles. Fig. S3 reveals a series of CV characterizations of (Au-pMBA) $@\text{SiO}_2$ NPs with the average silica thicknesses of 1.8 nm (A), 2.5 nm (B), 5 nm (C) and 6.5 nm (D) (Glassy carbon as working electrode, saturated calomel as reference electrode, platinum as auxiliary electrode and 0.1 mol·L⁻¹ H₂SO₄ as electrolyte).



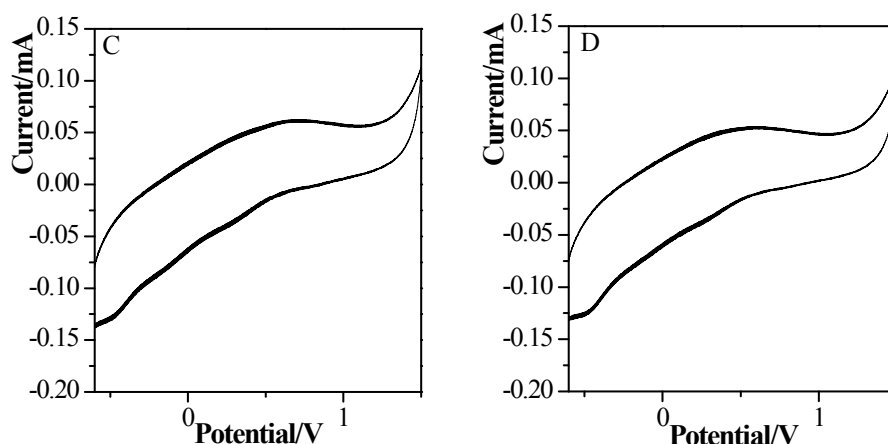


Fig. S3 CV characterizations of (Au-pMBA) $@\text{SiO}_2$ CSNPs synthesized using MPTMS as coupling agent with the silica thicknesses of 1.8 nm (A), 2.5 nm (B), 5 nm (C) and 6.5 nm (D).

For (Au-pMBA) $@\text{SiO}_2$ CSNPs, with the decrease of hydrolysis time of Na_2SiO_3 solution, the shell thickness will also decrease which may cause nonuniformity and discontinuity of the silica shells on the surfaces of gold NPs and further lead to the appearances of oxidation or reduction peaks of gold at 1.2 V or 0.8 V, respectively. But no evident peaks of gold are observed, stating that the whole particles are wholly-encapsulated except for the differences of shell thicknesses.

4. Measurements on pinhole effect of the films by SERS

In general, CV characterizations of (Au-pMBA) $@\text{SiO}_2$ films may not be sufficient to prove that the silica shells are compact and pinhole-free. Shell completeness is necessary but not sufficient condition of shell compactness. On the one hand, the generated tiny current may not be captured due to the detection sensitivity limitation of electrochemical workstation; on the other hand, even if there are tiny pinholes on the surfaces of silica shells, but the shells are still continuous on the whole which can isolate glassy carbon electrode from inner gold to avoid the redox reactions³. The common method to prove the compactness of the shells is pyridine (Py) pinhole testing⁴⁻⁶. As a kind of moderately-adsorbed probe molecule, Py possesses biggish scattering cross sections and easy-identified Raman characteristic

peaks, so it can be adsorbed on the surfaces of gold NPs but has very weak interaction forces with silica shells, and Py molecules will only be free around silica which will not generate any SERS signals; but once there are some tiny pinholes on the surfaces of silica shells, Py molecules will pass through the pinholes to be adsorbed on the surfaces of inner gold NPs by diffusion which will generate SERS signals³. For convenience, the monolayer film structures were selected instead of NP concentrated solutions to carry on Py pinhole testing, as shown in Fig. S4.

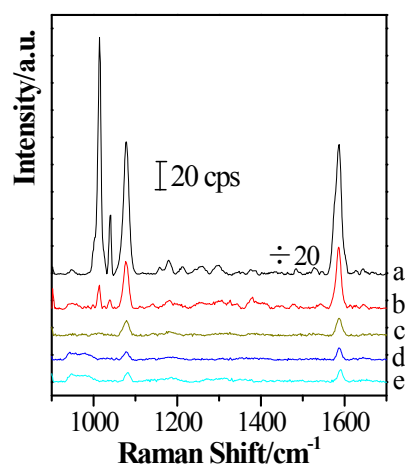


Fig. S4 Py pinhole testing of (Au-pMBA) $@SiO_2$ films of various silica shell thicknesses: 0 nm (a), 1.8 nm (b), 2.5 nm (c), 5 nm (d) and 6.5 nm (e).

For the previous SHINs pinhole testing, the absence of Py SERS signals can be considered as pinhole-free of silica shells and vice versa. But for (Au-pMBA) $@SiO_2$ NPs, some active adsorption sites of gold surfaces have been occupied by pMBA in advance, which blocked the adsorption of additional Py molecules. Therefore, the absence of Py signals was attributed to either pinhole-free of silica shells or the occupation of adsorption sites of pMBA. However, for naked (Au-pMBA) film without silica shells (Fig. S4 (a)), the SERS peaks at 1013 cm^{-1} and 1038 cm^{-1} which correspond to the ν_1 (ring breathing) and ν_{12} (symmetric trigonal ring breathing) modes of Py, respectively^{7,8}, are particularly obvious after being dropped on the silicon wafer. This result indicates that the occupation of pMBA on the surfaces of gold NPs in advance will not affect the interactions between subsequently-added Py

molecules and gold NPs, hence the absence of Py SERS signals can be considered as pinhole-free of silica shells without doubt. For (Au-pMBA)@1.8 nm SiO₂ film, weak Py signals can be observed indicating some tiny pinholes on the surfaces of 1.8 nm thin silica shells according to Fig. S4 (b). While for (Au-pMBA)@SiO₂ films whose silica shell thicknesses are no less than 2.5 nm, the disappearance of Py characteristic SERS peaks indicated the pinhole-free states for these thicker silica shells. In addition, the SERS peak intensity of pMBA for (Au-pMBA)@1.8 nm SiO₂ film decreases by at least 40 times compared with the one of (Au-pMBA) film for the sudden decrease of the electromagnetic field intensity as well as the hot spot coupling effect between the neighboring NPs due to the existence of silica shells⁹ and the increased gap distances. With the increase of silica shell thickness, the intensities further decrease to relatively stable values.

5. Line detections of (Au-pMBA)@SiO₂ films passing through the surfaces of GSCPs

Fig. S5 are the line detections of (Au-pMBA)@SiO₂ films passing through the surfaces of GSCPs with the silica shell thicknesses of 1.8 nm and 2.5 nm, respectively. (Excitation wavelength: 633 nm)

One can find that the SERS signal intensities of pMBA are several times higher in the areas on GSCPs than in the ones beyond GSCPs for either (Au-pMBA)@SiO₂ film. Meanwhile, there're few intensity differences for the same area of one film, which proves the uniformity of the films to a certain extent even when GSCPs are located under the films from the line detections.

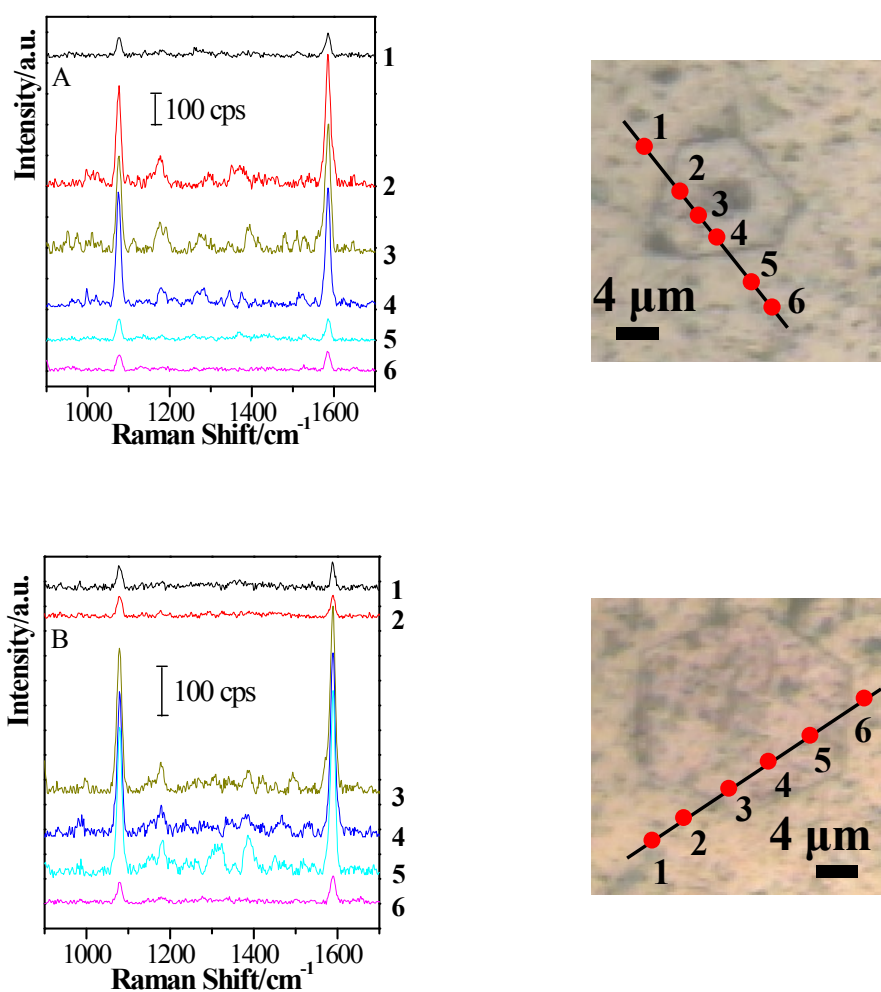


Fig. S5 SERS spectra of line detections of (Au-pMBA) $@\text{SiO}_2$ films on the surfaces of both GSCPs and silicon wafers of various silica shell thicknesses: 1.8 nm (A) and 2.5 nm (B). (Excitation wavelength: 633 nm)

References

- 1 J. F. Li, Core-shell nanoparticles-enhanced Raman spectroscopy[D]. *Xiamen: State key laboratory of physical chemistry of solid surfaces* 2010, 110-111.
- 2 B. Q. Zhang, S. B. Li, Q. Xiao, J. Li and J. J. Sun, *J. Raman Spectrosc.*, 2013, **44**, 1120-1125.
- 3 X. D. Lin, Studies on the synthesis, characterization and applications of core-shell nanoparticles with an ultra-thin shell[D]. *Xiamen: State key laboratory of physical chemistry of solid surfaces* 2013, 73-74.
- 4 X. D. Tian, B. J. Liu, J. F. Li, Z. L. Yang, B. Ren and Z. Q. Tian, *J. Raman Spectrosc.*, 2013, **44**, 994-998.
- 5 J. F. Li, S. B. Li, J. R. Anema, Z. L. Yang, Y. F. Huang, Y. Ding, Y. F. Wu, X. S. Zhou, D. Y. Wu, B. Ren, Z. L. Wang and Z. Q. Tian, *Appl. Spectrosc.*, 2011, **65**, 620-626.
- 6 V. Uzayisenga, X. D. Lin, L. M. Li, J. R. Anema, Z. L. Yang, Y. F. Huang, H. X. Lin, S. B. Li, J.

- F. Li and Z. Q. Tian, *Langmuir*, 2012, **28**, 9140-9146.
- 7 J. F. Li, A. Rudnev, Y. C. Fu, N. Bodappa and T. Wandlowski, *ACS NANO*, 2013, **7**, 8940-8952.
- 8 D. Y. Wu, X. M. Liu, S. Duan, X. Xu, B. Ren, S. H. Lin and Z. Q. Tian, *J. Phys. Chem. C*, 2008, **112**, 4195-4204.
- 9 M. Shanthil, R. Thomas, R. S. Swathi and K. G. Thomas, *J. Phys. Chem. Lett.*, 2012, **3**, 1459-1464.